Phase-dependent multiple optomechanically induced absorption in multimode optomechanical systems with mechanical driving

Cheng Jiang,* Yuanshun Cui, Xintian Bian, Fen Zuo, Hualing Yu, and Guibin Chen
School of Physics and Electronic Electrical Engineering, Huaiyin Normal University, 111 West Chang Jiang Road, Huai'an 223300, China
(Received 23 June 2016; published 22 August 2016)

We investigate theoretically the response of the output field from an optomechanical system consisting of N nearly degenerate mechanical resonators each coupled to a common cavity mode. When the cavity is driven simultaneously by a strong control field and a weak probe field and each mechanical resonator is driven by a coherent mechanical pump, we obtain the analytical expression for the probe transmission. We show that the probe transmission spectrum can exhibit multiple optomechanically induced absorption (OMIA) with at most N narrow absorption dips, which can be tuned by the phase and amplitude of the mechanical driving field as well as the control field. Moreover, it is shown that the peak probe transmission can be enhanced or suppressed by increasing the amplitude of the mechanical pump, which depends on the phase difference. This phase-dependent effect plays an important role in controlling the propagation of the probe field between OMIA and parametric amplification.

DOI: 10.1103/PhysRevA.94.023837

I. INTRODUCTION

The rapidly developing field of cavity optomechanics studies the interaction between the optical and mechanical degrees of freedom via radiation pressure. It provides an effective platform to observe quantum-mechanical behavior of macroscopic objects and has potential applications in ultrasensitive measurements and quantum information processing [1–3]. A generic optomechanical system consists of a Fabry-Pérot cavity where one mirror is fixed but another is free to move around its equilibrium position as a mechanical resonator. In the presence of a strong control field and a weak probe field, the electromagnetic response of the system is modified due to the radiation-pressure-induced mechanical oscillation, resulting in the phenomena of optomechanically induced transparency (OMIT) [4–11], optomechanically induced absorption (OMIA) [12–14], and parametric amplification [15] in various optomechanical systems. OMIT and OMIA are the optomechanical analogs of electromagnetically induced transparency (EIT) [16,17] and electromagnetically induced absorption (EIA) [18], which were first observed in atomic vapors and then in solid-state systems. Similar to EIT, OMIT can be used for controlling the group delay of light signals [19,20] and storing optical information in long-lived mechanical oscillations [21,22].

Moreover, more complicated interference effects appear if the mechanical resonator is driven by an additional coherent driving field. One unique advantage of the mechanical pump in optomechanical systems is that it can produce mechanical coherence directly, which is similar to generating atomic coherence in phaseonium systems by the direct drive at the microwave frequency [23]. Meanwhile, coherent oscillation of the mechanical resonator can be induced by the radiation pressure force at the beat frequency between the strong control field and weak probe field. The probe field can interfere with the control field scattered by the mechanical-pump-induced mechanical mode and radiation-pressure-induced mechanical mode. It is shown theoretically that the phase and amplitude of the mechanical pump can be used to control the probe transmission spectra [24,25], the group delay of the output probe field [26], and the process of second-order sideband generation [25,27]. Experimentally, cascaded optical transparency combined with extended optical delay and optical advancing have been demonstrated in a multimode-cavity optomechanical system by applying both an optical pump and a mechanical pump [28].

Recently, multimode optomechanical systems comprising more than two active degrees of freedom have attracted significant research interest [13,28–31]. On the one hand, by coupling two electromagnetic cavities with different resonant frequencies to a single mechanical resonator, one can realize frequency conversion between the two light fields [32–36]. On the other hand, a single electromagnetic cavity can couple with multiple mechanical resonators, leading to the hybridization between two mechanical modes [37], the preparation for the two-mode squeezed states [38], and the double OMIT phenomenon [39,40], which has also been investigated in an optomechanical system with a two-level atom [41]. In addition, Buchmann and Stamper-Kurn derived a general and complete master equation for the behavior of the two nondegenerate mechanical modes interacting via weak coupling to a common cavity field [42].

In this paper, we provide a theoretical study of a phase-dependent multiple OMIA phenomenon in a multimode optomechanical system in the presence of a strong coupling field, a weak probe field, and weak coherent mechanical driving fields. We demonstrate that there are at most N absorption dips in the probe transmission spectrum when the coupled system has N mechanical resonators with slightly different resonant frequencies. Furthermore, a detailed analysis shows that the probe transmission spectrum can be effectively tuned by the combination of the control field and the mechanical driving fields. In contrast to previous works about generic optomechanical systems with mechanical driving [24–27], in which only red sideband was considered, here we investigate

*chengjiang8402@163.com

the multiple OMIA and amplification in a general multimode optomechanical system driven on the blue sideband of the cavity.

II. MODEL AND THEORY

We consider an optomechanical system where N mechanical resonators with slightly different frequencies are individually coupled to a common cavity field, as shown in Fig. 1. In the microwave domain [see Fig. 1(a)], the microwave cavity may be described by an equivalent inductance L and an equivalent capacitance C; the bare resonance frequency of the cavity is then given by $\omega_0 = 1/\sqrt{LC}$ [7]. The motion of each mechanical resonator, expressed as time-varying capacitors C_k, independently modulates the total capacitance and therefore the resonance frequency of the cavity. The interaction is described by the Hamiltonian $\hat{H}_{\rm int} = \sum_{k=1}^{N} \hbar G_k \hat{x}_k \hat{a}^\dagger \hat{a}$, where $G_k = (\omega_0/2C)\partial C_k/\partial x_k$ denotes the change in the cavity resonance frequency for a given mechanical displacement $\hat{x}_k$ and $\hat{a}$ ($\hat{a}^\dagger$) is the annihilation (creation) operator of the cavity mode [15,20,30]. In the optical version [Fig. 1(b)], a multimode optomechanical system can be pictured as a Fabry-Pérot cavity containing N membranes. In both domains, we assume that the cavity is driven by a strong control field with frequency ω_c and a weak probe field with frequency

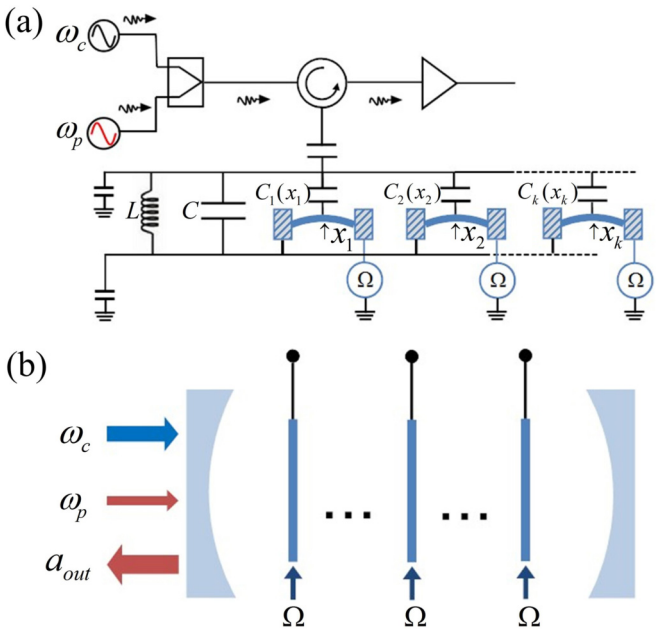

FIG. 1. Schematic diagram of the multimode optomechanical systems consisting of N mechanical resonators each coupled to a common cavity. The cavity is driven by a strong control field and a weak probe field, and each mechanical resonator is driven by a coherent mechanical pump at the beat frequency Ω between the probe field and control field. (a) Circuit optomechanical system with the microwave cavity represented by the equivalent inductance L and capacitance C. The displacement x_k of each mechanical resonator results in a time-varying capacitor C_k and independently modulates the total capacitance C and, hence, the cavity frequency. (b) Optomechanical system with N membranes placed inside an optical cavity.

ω_p simultaneously. Meanwhile, each mechanical resonator is driven by a weak coherent mechanical pump with amplitude ε_m, frequency $\Omega = \omega_p - \omega_c$, and phase ϕ_m. In a rotating frame at the frequency of the control field ω_c, the Hamiltonian of the multimode optomechanical system can be written as [29,30]

$$\hat{H} = \hbar\Delta_0 \hat{a}^\dagger \hat{a} + \sum_{k=1}^{N} \left(\frac{\hat{p}_k^2}{2m_k} + \frac{1}{2} m_k \omega_k^2 \hat{x}_k^2 \right) + \sum_{k=1}^{N} \hbar G_k \hat{x}_k \hat{a}^\dagger \hat{a} + \hat{H}_{dr}, \tag{1}$$

where $\Delta_0 = \omega_0 - \omega_c$ is the detuning of the control field from the bare cavity frequency ω_0. $\hat{x}_k$ and $\hat{p}_k$ are the displacement and momentum operators of the kth mechanical resonator having effective mass m_k and resonance frequency ω_k. $\hat{H}_{dr}$ describes the interaction between the optomechanical system and the driving fields [24–27]:

$$\hat{H}_{dr} = i\hbar\sqrt{\eta_c \kappa/2}[(\varepsilon_c + \varepsilon_p e^{-i\Omega t - i\phi_p})\hat{a}^\dagger - \text{H.c.}] - 2\sum_{k=1}^{N} \hat{x}_k \varepsilon_m \cos(\Omega t + \phi_m), \tag{2}$$

where κ is the total decay rate of the cavity and consists of an intrinsic decay rate κ_0 and external decay rate κ_{ex}. The coupling parameter $\eta_c = \kappa_{ex}/(\kappa_{ex} + \kappa_0)$ can be experimentally adjusted, and we choose $\eta_c = 1/2$ in this work. ε_c and ε_p are the amplitudes of the control field and the probe field, and they are related to their powers by $\sqrt{2P_c/\hbar\omega_c}$ and $\sqrt{2P_p/\hbar\omega_p}$, respectively. ϕ_p is the phase difference between the probe field and control field, and we have assumed that the frequency of the mechanical driving field is equal to the frequency detuning between the probe field and control field. Applying the Heisenberg equations of motion for the cavity and mechanical modes and neglecting the quantum noise and thermal noise terms [20], we have

$$\frac{d}{dt}\hat{a} = -\left[\kappa/2 + i\left(\Delta_0 + \sum_{k=1}^{N} G_k \hat{x}_k\right)\right]\hat{a} + \sqrt{\eta_c \kappa/2}(\varepsilon_c + \varepsilon_p e^{-i\Omega t - i\phi_p}), \tag{3}$$

$$\frac{d}{dt}\hat{x}_k = \frac{\hat{p}_k}{m_k}, \tag{4}$$

$$\frac{d}{dt}\hat{p}_k = -m_k\omega_k^2 \hat{x}_k - \hbar G_k \hat{a}^\dagger \hat{a} + 2\varepsilon_m \cos(\Omega t + \phi_m) - \gamma_k \hat{p}_k, \tag{5}$$

where the decay rates for the cavity (κ) and mechanical resonators (γ_k) have been introduced phenomenologically. We can obtain the steady-state solutions for the intracavity field and mechanical displacement by setting all the time derivatives in Eqs. (3)–(5) to be zero, which obeys the following algebraic equations:

$$\bar{a} = \frac{\sqrt{\eta_c \kappa/2}}{\kappa/2 + i\bar{\Delta}}\varepsilon_c, \tag{6}$$

$$m_k\omega_k^2 \bar{x}_k + \hbar G_k |\bar{a}|^2 = 0, \tag{7}$$

where $\bar{\Delta} = \Delta_0 + \sum_{k=1}^{N} G_k \bar{x}_k$ is the effective cavity detuning including radiation pressure effect.

Since the probe field is much weaker than the control field, we can rewrite each Heisenberg operator as the sum of its steady-state mean value and a small fluctuation, i.e., $\hat{a}(t) = \bar{a} + \delta\hat{a}(t)$ and $\hat{x}_k = \bar{x}_k + \delta\hat{x}_k(t)$. Then, keeping only first-order terms in the small quantities $\delta\hat{a}$, $\delta\hat{a}^\dagger$, and $\delta\hat{x}_k$, we can obtain the linearized Heisenberg-Langevin equations as follows:

$$\frac{d}{dt}\delta\hat{a}(t) = -(\kappa/2 + i\bar{\Delta})\delta\hat{a} - i\sum_{k}^{N} G_k\bar{a}\delta\hat{x}_k(t) + \sqrt{\eta_c\kappa/2}\varepsilon_p e^{-i(\Omega t+\phi_p)}, \quad (8)$$

$$\frac{d^2}{dt^2}\delta\hat{x}_k(t) + \gamma_k\frac{d}{dt}\delta\hat{x}_k(t) + \omega_k^2\delta\hat{x}_k(t) = -\frac{\hbar G_k}{m_k}\bar{a}[\delta\hat{a}(t) + \delta\hat{a}^\dagger(t)] + \frac{2\varepsilon_m}{m_k}\cos(\Omega t + \phi_m), \quad (9)$$

where the neglected nonlinear terms such as $\delta\hat{x}_k\delta\hat{a}$ and $\delta\hat{a}^\dagger\delta\hat{a}$ can result in second-order sidebands [8,27]. Note that the system is stable only if all the eigenvalues associated with the linearized equations (8) and (9) have negative real parts. The stability condition can be derived by applying the Routh-Hurwitz criterion [43], whose general form is too cumbersome to give here. However, we have checked numerically that the parameters we choose in this paper satisfy the stability condition. Since the drives are classical coherent fields, we will identify all the operators with their expectation values, viz., $\langle\delta\hat{a}(t)\rangle = \delta a(t)$ and $\langle\delta\hat{x}_k(t)\rangle = \delta x_k(t)$. In order to solve Eqs. (8) and (9) we introduce the following ansatz: $\delta a(t) = A^- e^{-i\Omega t} + A^+ e^{i\Omega t}$ and $\delta x_k(t) = X_k e^{-i\Omega t} + X_k^* e^{i\Omega t}$. We are interested here in the resolved sideband regime ($\kappa \ll \omega_k$) and close to the blue ($\bar{\Delta} = -\omega_m$) sideband of the control field, where ω_m is the average frequency of N mechanical resonators. In this case, the lower sideband A^+ is far off resonance and can be neglected. Upon substituting the above ansatz into Eqs. (8) and (9), we can obtain the amplitude A^- of the cavity field,

$$A^- = \frac{\sqrt{\eta_c\kappa/2}\varepsilon_p e^{-i\phi_p}}{\kappa/2 - i(\Omega+\omega_m) + \sum_k^N \hbar G_k^2|\bar{a}|^2\chi(m_k,\omega_k)} + \frac{\sum_k^N G_k\bar{a}\chi(m_k,\omega_k)\varepsilon_m e^{-i\phi_m}}{\kappa/2 - i(\Omega+\omega_m) + \sum_k^N \hbar G_k^2|\bar{a}|^2\chi(m_k,\omega_k)}, \quad (10)$$

where

$$\chi(m_k,\omega_k) = \frac{1}{2m_k\omega_k[-\gamma_k/2 + i(\Omega+\omega_k)]}. \quad (11)$$

The first term in Eq. (10) is the contribution from the probe and the control field, which gives rise to the usual optomechanically induced absorption and parametric amplification. The second term is the contribution from the phonon-photon parametric process involving the driving on the mechanical resonators.

The output field from the optomechanical cavity can be found using the input-output relationship

$$\begin{aligned} a_{\rm out}(t) &= a_{\rm in}(t) - \sqrt{\eta_c\kappa/2}a(t) \\ &= (\varepsilon_c - \sqrt{\eta_c\kappa/2}\bar{a})e^{-i\omega_c t} \\ &\quad + (\varepsilon_p e^{-i\phi_p} - \sqrt{\eta_c\kappa/2}A^-)e^{-i\omega_p t} \\ &\quad - \sqrt{\eta_c\kappa/2}A^+ e^{-i(2\omega_c-\omega_p)t}. \end{aligned} \quad (12)$$

Defining the transmission of the probe field as $t = (\varepsilon_p e^{-i\phi_p} - \sqrt{\eta_c\kappa/2}A^-)/(\varepsilon_p e^{-i\phi_p})$, we can get

$$t = t_1 + t_2, \quad (13)$$

with

$$t_1 = 1 - \frac{\eta_c\kappa/2}{\kappa/2 - i(\Omega+\omega_m) + \sum_k^N \hbar G_k^2|\bar{a}|^2\chi(m_k,\omega_k)}, \quad (14)$$

$$t_2 = -\frac{\sqrt{\eta_c\kappa/2}\sum_k^N G_k\bar{a}\chi(m_k,\omega_k)\varepsilon_m/\varepsilon_p e^{-i\phi}}{\kappa/2 - i(\Omega+\omega_m) + \sum_k^N \hbar G_k^2|\bar{a}|^2\chi(m_k,\omega_k)}, \quad (15)$$

where $\phi = \phi_m - \phi_p$ is the phase difference between two sources. t_1 is the expression for the probe transmission without mechanical pump, which has been discussed in previous work with a single mechanical resonator [12]. t_2 represents the modification of the probe transmission induced by the mechanical driving field. Interference between t_1 and t_2 determines the probe transmission spectrum, in which the control power P_c, the phase difference ϕ, and the amplitude ε_m of the mechanical driving field play an important role.

III. RESULTS AND DISCUSSION

In this section, we will numerically investigate the transmission spectrum of the probe field when the common cavity field is coupled to N mechanical resonators. For simplicity, we first consider the optomechanical systems with two mechanical resonators with slightly different frequencies. The parameters used are chosen from a recent experiment [30]: $\omega_0 = 2\pi \times 6.98$ GHz, $\omega_1 = 2\pi \times 32.1$ MHz, $\omega_2 = 2\pi \times 32.5$ MHz, $\kappa = 2\pi \times 6.2$ MHz, $\gamma_1 = \gamma_2 = \gamma_m = 2\pi \times 930$ Hz, $m_1 = 557$ fg, $m_2 = 534$ fg, $G_1 = 2\pi \times 1.8$ MHz/nm, $G_2 = 2\pi \times 2$ MHz/nm. Here and below, we consider only the situation where the cavity field is driven on its blue sideband ($\bar{\Delta} = -\omega_m$).

In the absence of mechanical driving, the probe transmission $|t|^2$ is plotted as a function of $(\Omega+\omega_1)/2\pi$ for $P_c = 2$ nW in Fig. 2. We can see that there are two very narrow absorption dips in the center of the figure, and the insets show clearly that the two dips locate at $(\Omega+\omega_1)/2\pi = 0$ and $(\Omega+\omega_1)/2\pi = -0.4$ MHz. Using the chosen values of the mechanical resonance frequencies, we can find that the two absorption dips locate, respectively, at $\Omega = -\omega_1$ and $\Omega = -\omega_2$ in the probe transmission, which can be called double optomechanically induced absorption. Similar to the single OMIA in other optomechanical systems [6,12], this phenomenon can be understood as a result of a radiation pressure force at the beat frequency Ω between the probe and control photons. When this frequency difference is close to the mechanical resonance frequency, $\Omega = -\omega_k$ ($k = 1,2$), the mechanical mode starts to vibrate coherently, generating

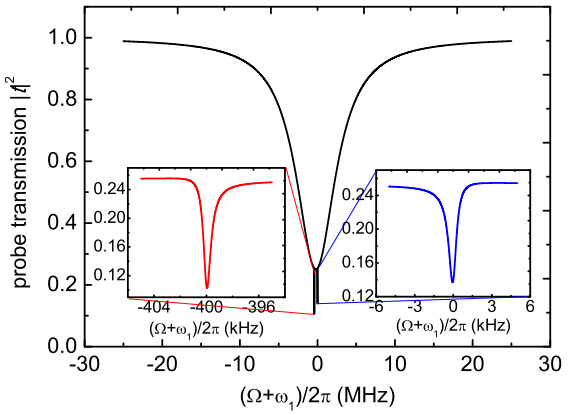

FIG. 2. Probe transmission versus the probe detuning $(\Omega + \omega_1)/2\pi$ without mechanical driving when the control field is blue detuned by the amount of $\omega_m = (\omega_1 + \omega_2)/2$ with $P_c = 2$ nW. The insets show the two sharp absorption dips close to $\Omega = -\omega_1$ and $\Omega = -\omega_2$ on an enlarged scale. Other parameters are $\omega_0 = 2\pi \times 6.98$ GHz, $\omega_1 = 2\pi \times 32.1$ MHz, $\omega_2 = 2\pi \times 32.5$ MHz, $\kappa = 2\pi \times 6.2$ MHz, $\eta_c = 0.5$, $\gamma_1 = \gamma_2 = \gamma_m = 2\pi \times 930$ Hz, $m_1 = 557$ fg, $m_2 = 534$ fg, $G_1 = 2\pi \times 1.8$ MHz/nm, $G_2 = 2\pi \times 2$ MHz/nm. We fix $\varepsilon_p = \varepsilon_c/1000$ throughout this work since the probe field should be much weaker than the control field; otherwise, the perturbation method will be invalid.

Stokes and anti-Stokes scattering of light from the strong control field. If the cavity is driven on its blue sideband $(\omega_0 - \omega_c \approx -\omega_m)$ and the system operates in the resolved-sideband regime ($\omega_1 > \kappa$ and $\omega_2 > \kappa$), the anti-Stokes field at $\omega_c + \omega_k$ is strongly suppressed because it is off resonant with the cavity field and we can assume only the Stokes field at $\omega_c - \omega_k$ builds up within the cavity. Furthermore, constructive interference between the Stokes field and the degenerate probe field can enhance the buildup of the intra-cavity probe field. The increased absorption of probe photons into the cavity manifests itself as the reduced probe transmission at $\Omega = -\omega_1$ and $\Omega = -\omega_2$. It should be noted that there is only a single absorption dip when the two mechanical resonators have the same resonance frequency and no direct interaction.

In the rest of the paper, we mainly investigate the effect of mechanical driving on the transmission spectrum of the probe field. Here we assume for simplicity that each mechanical resonator is driven by a coherent mechanical pump with the same amplitude ε_m, frequency Ω, and phase ϕ_m. In general, each mechanical resonator can be driven independently. It is shown in Fig. 2 that there are two absorption dips in the probe transmission. Without loss of generality, we just need to focus on investigating one absorption dip and the other should be similar. It should be pointed out that those two mechanical modes are separated by a frequency much larger than the mechanical damping rate γ_m so that the two absorption dips don't overlap. Figure 3 plots the peak probe transmission $|t_p|^2$ at $\Omega = -\omega_1$ (i.e., $|t_p|^2 = |t|^2_{\Omega=-\omega_1}$) as a function of phase difference ϕ and amplitude ε_m of the external driving force under the same control power $P_c = 2$ nW. It can be seen that with the increase of the driving amplitude, the effect of phase difference ϕ on the peak probe transmission $|t_p|^2$ becomes more evident. The peak probe transmission $|t_p|^2$ reaches the

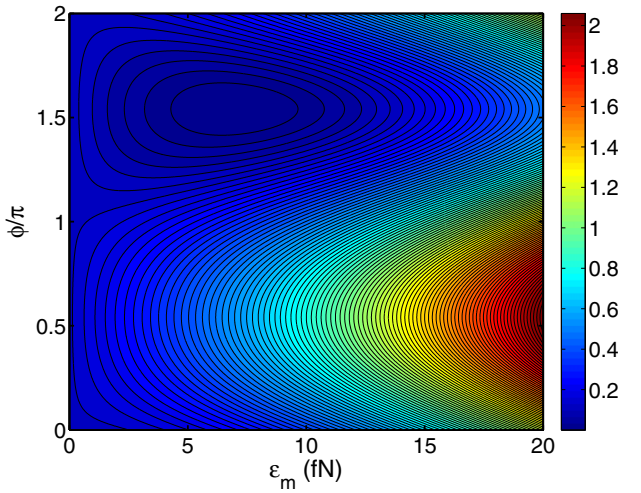

FIG. 3. Contour plot of the peak probe transmission $|t_p|^2$ at $\Omega = -\omega_1$ as a function of phase difference ϕ and amplitude ε_m of the external driving force for a constant control power $P_c = 2$ nW. Other parameters are the same as in Fig. 2.

maximum near $\phi = \pi/2$ and the minimum near $\phi = 3\pi/2$ under the same amplitude ε_m, which can be explained by the process of interference. Moreover, it is shown that the peak probe transmission can exceed 1 when ε_m becomes larger than a critical value in a certain range of phase difference. Therefore, the system can easily switch from double OMIA to parametric amplification by controlling the phase and amplitude of the mechanical driving force.

In order to see the effect of mechanical driving more clearly, we plot the probe transmission spectra versus probe detuning $(\Omega + \omega_1)/2\pi$ with different mechanical pumps in Fig. 4. In the case without the mechanical driving ($\varepsilon_m = 0$), there is a reduced probe transmission $|t|^2$ at $\Omega = -\omega_1$. When the mechanical driving force is applied to the mechanical resonator with $\varepsilon_m = 12$ fN, the probe transmission is greatly

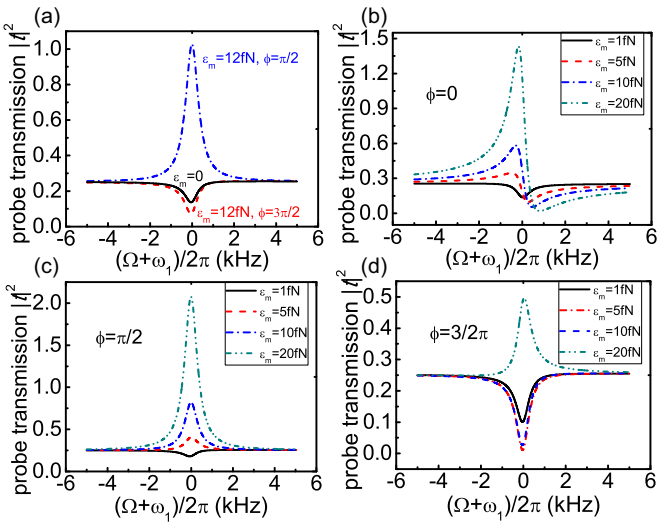

FIG. 4. Probe transmission spectra as a function of probe detuning $(\Omega - \omega_1)/2\pi$ with different values of ε_m and ϕ. Other parameters are the same as in Fig. 2.

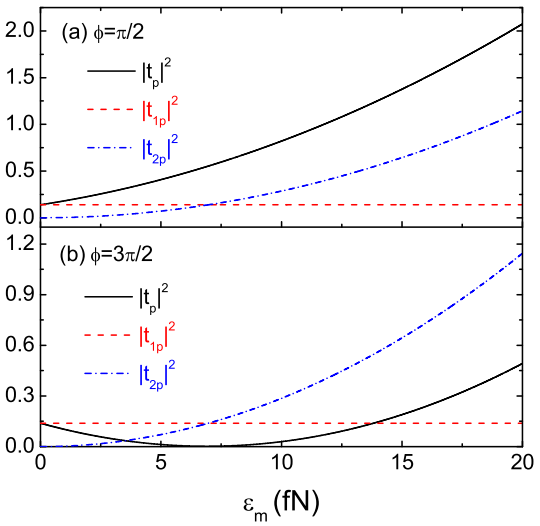

FIG. 5. Plots of $|t_p|^2$, $|t_{1p}|^2$, and $|t_{2p}|^2$ at $\Omega = -\omega_1$ as a function of the mechanical driving force ε_m for (a) $\phi = \pi/2$ and (b) $\phi = 3\pi/2$. Other parameters are the same as in Fig. 2.

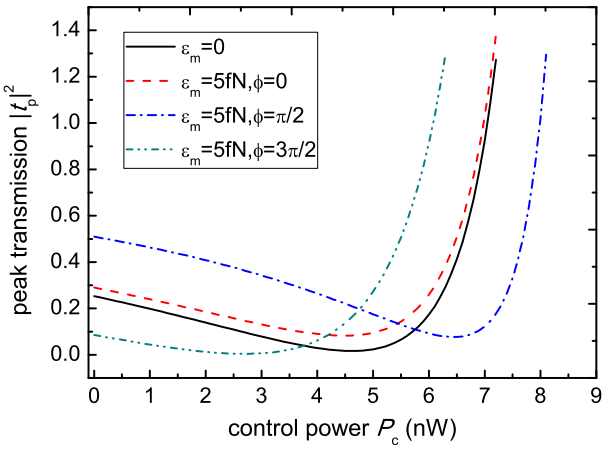

FIG. 6. Peak probe transmission $|t_p|^2$ at $\Omega = -\omega_1$ as a function of the control power P_c. The four curves correspond to the case without mechanical driving ($\varepsilon_m = 0$) and with mechanical driving of the same amplitude ($\varepsilon_m = 5$ fN) but different phases ($\phi = 0$, $\pi/2$, and $3\pi/2$, respectively). Other parameters are the same as in Fig. 2.

enhanced for $\phi = \pi/2$ or further reduced for $\phi = 3\pi/2$, as shown in Fig. 4(a). Hence, the phase-dependent effect is quite evident. Figures 4(b)–4(d) present the transmission spectra as a function of $(\Omega + \omega_1)/2\pi$ for different amplitudes of the mechanical driving with $\phi = 0$, $\phi = \pi/2$, and $\phi = 3\pi/2$, respectively. When $\phi = 0$ and $\phi = \pi/2$, the peak probe transmission at $\Omega = -\omega_1$ is enhanced monotonically by increasing the amplitude of the mechanical driving. However, increasing the amplitude of the mechanical driving does not always bring an enhancement of the probe transmission when $\phi = 3\pi/2$. If the mechanical driving is weak, $\varepsilon_m \leqslant 7$ fN, for example, the peak probe transmission decreases with the increase of ε_m, but when ε_m is further increased to 20 fN, we can see that the peak probe transmission is enhanced. Such a phase-dependent effect makes the probe transmission spectrum more tunable in optomechanical systems with mechanical driving.

To gain a more physical origin for the above phase-dependent effects, we plot $|t_p|^2$, $|t_{1p}|^2$, and $|t_{2p}|^2$ at $\Omega = -\omega_1$ (i.e., $|t_{1p}|^2 = |t_1|^2_{\Omega=-\omega_1}$ and $|t_{2p}|^2 = |t_2|^2_{\Omega=-\omega_1}$) versus the mechanical driving force ε_m in Fig. 5. $|t_{1p}|^2$ stays constant, but $|t_{2p}|^2$ increases monotonically with the enhancement of ε_m. When $\phi = \pi/2$, constructive interference occurs between t_{1p} and t_{2p}. If they have the same amplitude, perfect constructive interference leads to the result that $|t_p|^2 \simeq 4|t_{1p}|^2 = 4|t_{2p}|^2$ around $\varepsilon_m = 7$ fN, as shown in Fig. 5(a). When $\phi = 3\pi/2$, there is destructive interference between t_{1p} and t_{2p}, and it can be seen from Fig. 5(b) that $|t_p|^2 \simeq 0.0023$ around $\varepsilon_m = 7$ fN, where perfect destructive interference occurs and the energy of photons are transferred into the mechanical degrees of freedom. Moreover, Figs. 5(a) and 5(b) also show that the larger the difference between the amplitudes of t_{1p} and t_{2p} is, the weaker the interference effect becomes.

The control field is kept constant in the above discussions, i.e., $\bar{\Delta} = -\omega_m$ and $P_c = 2$ nW. In Fig. 6, the peak probe transmission $|t_p|^2$ at $\Omega = -\omega_1$ is plotted as a function of control power with different mechanical pumps. In the four cases, the effect of control power is similar. At first, the peak probe transmission decreases with increasing control power from an initial value for the bare cavity to a minimum, but further increasing the control power will make $|t_p|^2$ increase again and exceed the initial value for the bare cavity. If the control power is strong enough, $|t_p|^2$ can even be larger than 1, which indicates that the system enters the regime of parametric amplification. However, it can be seen that the effect of phase difference on the peak probe transmission is evident when the amplitude of the mechanical driving remains the same. The curve for $\varepsilon_m = 5$ fN and $\phi = 0$ is similar to the curve without the mechanical driving, but some remarkable differences exist when $\phi = \pi/2$ and $\phi = 3\pi/2$. We give some physical insight into these phenomena as follows: both radiation pressure and mechanical driving can result in the coherent oscillation of mechanical resonators, giving rise to two kinds of Stokes scattering of light from the control field. Phase difference ϕ plays an important role in the interference between these two Stokes fields and intracavity probe field. Moreover, the number of Stokes photons (i.e., down-converted control photons) is dependent on the control power P_c. If the control power P_c is low enough, the number of down-converted control photons is smaller than the number of probe photons sent to the cavity. Therefore, the stimulated absorption of probe photons caused by the interference effect is only partial. With the increase of the control power, the absorption dip deepens and minimum probe transmission can be obtained when the number of down-converted control photons is equal to the number of probe photons. If the control power is further increased, the number of down-converted control photons exceeds the number of probe photons, leading to an increase in the probe transmission. When the control power is bigger than a critical value, which depends on the system parameters as well as the phase and magnitude of the mechanical pump, the probe transmission can exceed unity [12]. Note that the probe power increases simultaneously with the increasing of the control power since we fix $\varepsilon_p = \varepsilon_c/1000$ but ε_m doesn't change; thus, the contribution from the two terms in Eq. (10)

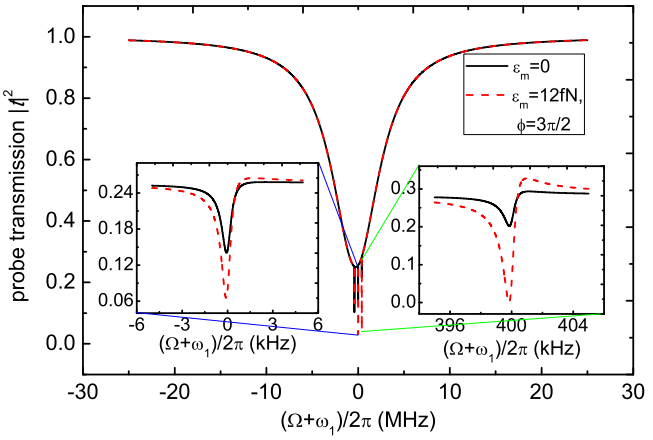

FIG. 7. Probe transmission $|t|^2$ versus the probe detuning $(\Omega + \omega_1)/2\pi$ considering the effect of mechanical driving. The control field is blue detuned by the amount of $\omega_m = (\omega_1 + \omega_2 + \omega_3)/3$ with $P_c = 2$ nW. The insets show the two sharp absorption dips close to $\Omega = -\omega_1$ and $\Omega = -\omega_3$ on an enlarged scale. Parameters for the third mechanical resonator are $\omega_3 = 2\pi \times 31.7$ MHz, $m_3 = 580$ fg, $G_3 = 2\pi \times 1.6$ MHz/nm, $\gamma_3 = 2\pi \times 930$ Hz. Other parameters are the same as in Fig. 2.

also varies with the control power, and there is a crossing point between the two curves for $\phi = \pi/2$ and $\phi = 3\pi/2$.

Next, we consider a multimode optomechanical system with three different mechanical resonators coupled to a common cavity field. Based on the current experimental parameters [30], we assume the parameters of the third mechanical resonator are as follows: $\omega_3 = 2\pi \times 31.7$ MHz, $m_3 = 580$ fg, $G_3 = 2\pi \times 1.6$ MHz/nm, $\gamma_3 = 2\pi \times 930$ Hz. Figure 7 shows the probe transmission $|t|^2$ against the probe detuning $(\Omega + \omega_1)/2\pi$ before and after the mechanical driving forces are applied. There are three absorption dips at the bottom of the transmission spectrum, which locate at $\Omega = -\omega_1$, $\Omega = -\omega_2$, and $\Omega = -\omega_3$, respectively. Moreover, the effect of mechanical driving is similar to the case with two mechanical resonators, as shown in the insets Fig. 7.

We have shown that double and triple optomechanically induced absorption exist in optomechanical systems with two and three nondegenerate mechanical resonators, respectively. Finally, in the general multimode optomechanical system with N mechanical modes, if all the frequencies of the N mechanical resonators are slightly different, we can conclude qualitatively that there are at most N absorption dips at $\Omega = -\omega_k (k = 1,2,3,\ldots,N)$. The physical reason can also be understood in terms of interference effects between the probe field and the generated Stokes field at the frequency $\omega_c - \omega_k (k = 1,2,3,\ldots,N)$, which has been explained in detail before. If $L (1 < L < N)$ mechanical resonators have the same frequency ω $(\omega_1 = \omega_2 = \cdots = \omega)$ and the frequencies of the left $N - L$ resonators are different from ω, there are $N - L + 1$ absorption dips in the probe transmission spectrum. However, if all the mechanical resonators have the same frequency $\omega_k = \omega_m$, only one absorption dip exists when $\Omega = -\omega_m$. Experimentally, coupling multiple mechanical resonators to a common cavity can be realized by using the on-circuit implementation of the optomechanical interaction in the microwave domain [30] or trapping several distinguishable atomic ensembles within the same optical resonator [44]. Note that collective effects in multimode optomechanics have attracted some attention in recent years. For example, Kipf and Agarwal have theoretically shown that the system's response can be switched from a superradiant regime to a collective gain regime by varying the frequency detuning of the pump field [45]. Zhang *et al.* experimentally demonstrated that arrays of mechanical oscillators can be synchronized to oscillate in tandem when coupled purely through a common optical cavity field [46].

IV. CONCLUSION

In summary, we have explored the response of an optomechanical system which includes N nearly degenerate mechanical resonators to a weak probe field in the presence of a strong control field and weak mechanical driving fields. When the cavity was driven on its blue sideband, we obtained the analytical expression for the transmission of the probe field. We have shown that the system can exhibit the phenomenon of multiple OMIA with at most N narrow absorption dips, which can be adjusted by the amplitude and phase of the mechanical driving field. At low control power, the amplitude and phase of the mechanical pump can be used to control the system between OMIA and parametric amplification. Moreover, at high control power, parametric amplification of the weak probe field can also be obtained, in which the phase-dependent effect is evident.

ACKNOWLEDGMENTS

The authors gratefully acknowledge support from the National Natural Science Foundation of China (Grant No. 11304110), the Natural Science Foundation of Jiangsu Province (Grant No. BK20130413), the Natural Science Foundation of the Jiangsu Higher Education Institutions of China (Grants No. 13KJB140002 and No. 15KJB460004), and the Science and Technology Support Program of Huai'an City (Grant No. HAG2014019).

[1] T. J. Kippenberg and K. J. Vahala, Science **321**, 1172 (2008).
[2] F. Marquardt and S. M. Girvin, Physics **2**, 40 (2009).
[3] M. Aspelmeyer, T. J. Kippenberg, and F. Marquardt, Rev. Mod. Phys. **86**, 1391 (2014).
[4] G. S. Agarwal and S. Huang, Phys. Rev. A **81**, 041803 (2010).
[5] S. Weis, R. Rivière, S. Deléglise, E. Gavartin, O. Arcizet, A. Schliesser, and T. J. Kippenberg, Science **330**, 1520 (2010).
[6] A. H. Safavi-Naeini, T. P. Mayer Alegre, J. Chan, M. Eichenfield, M. Winger, Q. Lin, J. T. Hill, D. E. Chang, and O. Painter, Nature (London) **472**, 69 (2011).

[7] J. D. Teufel, D. Li, M. S. Allman, K. Cicak, A. J. Sirois, J. D. Whittaker, and R. W. Simmonds, Nature (London) **471**, 204 (2011).
[8] H. Xiong, L. G. Si, A. S. Zheng, X. X. Yang, and Y. Wu, Phys. Rev. A **86**, 013815 (2012).
[9] M. Karuza, C. Biancofiore, M. Bawaj, C. Molinelli, M. Galassi, R. Natali, P. Tombesi, G. Di Giuseppe, and D. Vitali, Phys. Rev. A **88**, 013804 (2013).
[10] A. Kronwald and F. Marquardt, Phys. Rev. Lett. **111**, 133601 (2013).
[11] H. Jing, S. K. Özdemir, Z. Geng, J. Zhang, X. Y. Lü, B. Peng, L. Yang, and F. Nori, Sci. Rep. **5**, 9663 (2015).
[12] F. Hocke, X. Zhou, A. Schliesser, T. J. Kippenberg, H. Huebl, and R. Gross, New J. Phys. **14**, 123037 (2012).
[13] K. N. Qu and G. S. Agarwal, Phys. Rev. A **87**, 031802 (2013).
[14] V. Singh, S. J. Bosman, B. H. Schneider, Y. M. Blanter, A. Castellanos-Gomez, and G. A. Steele, Nat. Nanotechnol. **9**, 820 (2014).
[15] F. Massel, T. T. Heikkilä, J.-M. Pirkkalainen, S. U. Cho, H. Saloniemi, P. Hakonen, and M. A. Sillanpää, Nature (London) **480**, 351 (2011).
[16] M. Fleischhauer, A. Imamoglu, and J. P. Marangos, Rev. Mod. Phys. **77**, 633 (2005).
[17] Y. Wu and X. X. Yang, Phys. Rev. A **71**, 053806 (2005).
[18] A. M. Akulshin, S. Barreiro, and A. Lezama, Phys. Rev. A **57**, 2996 (1998).
[19] C. Jiang, H. X. Liu, Y. S. Cui, X. W. Li, G. B. Chen, and B. Chen, Opt. Express **21**, 12165 (2013).
[20] X. Zhou, F. Hocke, A. Schliesser, A. Marx, H. Huebl, R. Gross, and T. J. Kippenberg, Nat. Phys. **9**, 179 (2013).
[21] D. E. Chang, A. H. Safavi-Naeini, M. Hafezi, and O. Painter, New J. Phys. **13**, 023003 (2011).
[22] V. Fiore, Y. Yang, M. C. Kuzyk, R. Barbour, L. Tian, and H. L. Wang, Phys. Rev. Lett. **107**, 133601 (2011).
[23] M. O. Scully, S. Y. Zhu, and A. Gavrielides, Phys. Rev. Lett. **62**, 2813 (1989).
[24] W. Z. Jia, L. F. Wei, Y. Li, and Y. X. Liu, Phys. Rev. A **91**, 043843 (2015).
[25] J. Y. Ma, C. You, L. G. Si, H. Xiong, J. H. Li, X. X. Yang, and Y. Wu, Sci. Rep. **5**, 11278 (2015).
[26] X. W. Xu and Y. Li, Phys. Rev. A **92**, 023855 (2015).
[27] H. Suzuki, E. Brown, and R. Sterling, Phys. Rev. A **92**, 033823 (2015).
[28] L. Fan, K. Y. Fong, M. Poot, and H. X. Tang, Nat. Commun. **6**, 5850 (2015).
[29] H. Seok, L. F. Buchmann, E. M. Wright, and P. Meystre, Phys. Rev. A **88**, 063850 (2013).
[30] F. Massel, S. U. Cho, J.-M. Pirkkaleinen, P. J. Hakonen, T. T. Heikkilä, and M. A. Sillanpää, Nat. Commun. **3**, 987 (2012).
[31] X. W. Xu, Y. Li, A. X. Chen, and Y. X. Liu, Phys. Rev. A **93**, 023827 (2016).
[32] J. T. Hill, A. H. Safavi-Naeini, J. Chan, and O. Painter, Nat. Commun. **3**, 1196 (2012).
[33] Y. Liu, M. Davanco, V. Aksyuk, and K. Srinivasan, Phys. Rev. Lett. **110**, 223603 (2013).
[34] R. W. Andrews, R. W. Peterson, T. P. Purdy, K. Cicak, R. W. Simmonds, C. A. Regal, and K. W. Lehnert, Nat. Phys. **10**, 321 (2014).
[35] C. Dong, V. Fiore, M. C. Kuzyk, L. Tian, and H. Wang, Ann. Phys. (Berlin) **527**, 100 (2015).
[36] F. Lecocq, J. B. Clark, R. W. Simmonds, J. Aumentado, and J. D. Teufel, Phys. Rev. Lett. **116**, 043601 (2016).
[37] A. B. Shkarin, N. E. Flowers-Jacobs, S. W. Hoch, A. D. Kashkanova, C. Deutsch, J. Reichel, and J. G. E. Harris, Phys. Rev. Lett. **112**, 013602 (2014).
[38] M. J. Woolley and A. A. Clerk, Phys. Rev. A **89**, 063805 (2014).
[39] S. M. Huang, J. Phys. B. **47**, 055504 (2014).
[40] P. C. Ma, J. Q. Zhang, Y. Xiao, M. Feng, and Z. M. Zhang, Phys. Rev. A **90**, 043825 (2014).
[41] H. Wang, X. Gu, Y. X. Liu, A. Miranowicz, and F. Nori, Phys. Rev. A **90**, 023817 (2014).
[42] L. F. Buchmann and D. M. Stamper-Kurn, Phys. Rev. A **92**, 013851 (2015).
[43] E. X. DeJesus and C. Kaufman, Phys. Rev. A **35**, 5288 (1987).
[44] T. Botter, D. W. C. Brooks, S. Schreppler, N. Brahms, and D. M. Stamper-Kurn, Phys. Rev. Lett. **110**, 153001 (2013).
[45] T. Kipf and G. S. Agarwal, Phys. Rev. A **90**, 053808 (2014).
[46] M. Zhang, S. Shah, J. Cardenas, and M. Lipson, Phys. Rev. Lett. **115**, 163902 (2015).